



# A novel *Bacillus subtilis* BPM12 with high bis(2 hydroxyethyl)terephthalate hydrolytic activity efficiently interacts with virgin and mechanically recycled polyethylene terephthalate

Brana Pantelic<sup>a</sup>, Jeovan A. Araujo<sup>b</sup>, Sanja Jeremic<sup>a</sup>, Muhammad Azeem<sup>b</sup>, Olivia A. Attallah<sup>b,c</sup>, Romanos Siaperas<sup>d</sup>, Marija Mojicevic<sup>b</sup>, Yuanyuan Chen<sup>b</sup>, Margaret Brennan Fournet<sup>b</sup>, Evangelos Topakas<sup>d</sup>, Jasmina Nikodinovic-Runic<sup>a,\*</sup>

<sup>a</sup> Institute of Molecular Genetics and Genetic Engineering, University of Belgrade, Vojvode Stepe 444a, 11042 Belgrade 152, Serbia

<sup>b</sup> PRISM Research Institute, Technological University of the Shannon Midlands Midwest, Athlone, N37HD68, Ireland

<sup>c</sup> Pharmaceutical Chemistry Department, Faculty of Pharmacy, Heliopolis University, Cairo - Belbeis Desert Road, El Salam, Cairo 11777, Egypt

<sup>d</sup> Industrial Biotechnology & Biocatalysis Group, Biotechnology Laboratory, School of Chemical Engineering, National Technical University of Athens, Iroon Polytechniou 9, 15772, Athens, Greece

## ARTICLE INFO

### Article history:

Received 3 April 2023

Received in revised form 22 July 2023

Accepted 25 July 2023

Available online 29 July 2023

### Keywords:

Polyethylene terephthalate (PET)

Recycling

Biocatalysis

*Bacillus*

BHET-ase

Carboxylesterase

## ABSTRACT

Biotechnological treatment of plastic waste has gathered substantial attention as an efficient and generally greener approach for polyethylene terephthalate (PET) depolymerization and upcycling in comparison to mechanical and chemical processes. Nevertheless, a suitable combination of mechanical and microbial degradation may be the key to bringing forward PET upcycling. In this study, a new strain with an excellent bis(2 hydroxyethyl)terephthalate (BHET) degradation potential (1000 mg/mL in 120 h at 30 °C) and wide temperature (20–47 °C) and pH (5–10) tolerance was isolated from a pristine soil sample. It was identified as *Bacillus subtilis* BPM12 via phenotypical and genome analysis. A number of enzymes with potential polymer degrading activities were identified, including carboxylesterase BPM12CE that was efficiently expressed both, homologously in *B. subtilis* BPM12 and heterologously in *B. subtilis* 168 strain. Overexpression of this enzyme enabled *B. subtilis* 168 to degrade BHET, while the activity of BPM12 increased up to 1.8-fold, confirming its BHET-ase activity. Interaction of *B. subtilis* BPM12 with virgin PET films and films that were re-extruded up to 5 times mimicking mechanical recycling, revealed the ability of the strain to attach and form biofilm on each surface. Mechanical recycling resulted in PET materials that are more susceptible to chemical hydrolysis, however only slight differences were detected in biological degradation when BPM12 whole-cells or cell-free enzyme preparations were used. Mixed mechano/bio-degradation with whole-cells and crude enzyme mixes from this strain can serve to further increase the percentage of PET- based plastics that can enter circularity.

© 2023 The Author(s). Published by Elsevier B.V. This is an open access article under the CC BY-NC-ND license (<http://creativecommons.org/licenses/by-nc-nd/4.0/>).

\* Corresponding author.

E-mail address: [jasmina.nikodinovic@imgge.bg.ac.rs](mailto:jasmina.nikodinovic@imgge.bg.ac.rs) (J. Nikodinovic-Runic).

## 1. Introduction

In the last decade, global plastic production reached over 360 million tons annually (Magalhães et al., 2021). Plastic pollution has become the focus of numerous scientific studies and industry lead-efforts (Laskar and Kumar, 2019). However, the solution for efficient large-scale plastic degradation/regeneration and recycling remains elusive. Further exaggerating the environmental impacts, plastic production uses about 8% of the world's fossil fuel resources, releasing greenhouse gasses and contributing to global warming (Samak et al., 2020). Europe is the leader in plastic recycling, with close to 29 million tons of post-consumer plastics collected out of 55 million tons produced in 2020. However, only 34.6% of collected materials were recycled while 42% were incinerated for energy recovery and 23.4% were landfilled (PlasticsEurope, 2021). Hence, additional research is needed to develop efficient strategies for tackling the problem of plastic waste accumulation and its adverse effects on the environment and health.

Polyethylene terephthalate (PET) is a synthetic polyester with a heteroatomic backbone made by reacting ethylene glycol (EG) and terephthalic acid (TPA). It represents 8.4% (w/w) of the total plastic produced and it is mainly used for beverage bottles (Kosiorowska et al., 2022). Efficient PET recovery of high-grade PET waste, such as beverage bottles, has been developed to provide "clean" and "high purity" PET waste streams for recycling. Recovered PET can undergo re-extrusion (enabling recovery of uncontaminated PET scraps in manufacturing plants), mechanical recycling (reprocessing PET into granules via extrusion processes yielding PET with reduced performances), chemical recycling (a variety of chemical processes for the depolymerization of PET and subsequent repolymerization into new polymers) and energy recovery (Benyathiar et al., 2022). Recycled PET is a commodity with many end uses, for the benefit of society and the environment. Traditionally mechanical recycling is the most widely used method of PET recycling and its application is likely to increase in the following years due to its low energy consumption and absence of use of hazardous chemical reagents (Suzuki et al., 2022). Rules have been adopted to ensure that recycled plastic can be safely used in food packaging and contribute to the overall sustainability towards achieving the objectives of the Circular Economy Action Plan (Commission, 2022). Processing including solid state polycondensation (SSP) can increase molecular weight and achieve parameters required to produce food contact approved PET according to regulation (EU) No 10/2011 and No 64/201. On the other side, chemical recycling can be applied to a wider range of mixed plastic waste but in many cases carries the burden of involving additional harmful chemicals and costs in the processes. Through chemical recycling, even multilayer colored PET plastic waste can be depolymerized into its main building blocks, allowing repolymerization following arduous purification or in the case of polyolefins, liquefaction through a thermo-chemical process can be used for conversion into products similar to crude oil (Ragaert et al., 2017). Therefore, milder conditions for chemical recycling and combination with other lower carbon means of polymer depolymerization should be explored.

In contrast to mechanical and chemical recycling, biocatalysis has emerged as an environmentally friendly and efficient approach for PET recycling (Nguyen et al., 2023; Wei and Zimmermann, 2017). The ester bonds which make up the backbone of the polyester polymer are susceptible to enzymatic degradation via hydrolysis by a number of enzymes with esterase activities, including PETases, lipases, cutinases and carboxylesterases (Jaiswal et al., 2020; Nikolaivits et al., 2022). The highly hydrophobic PET polymer is broken down into a variety of largely soluble oligomer degradation intermediates during enzymatic degradation. Through a series of endo- and exo- cleavages of ester bonds, products such as bis(2-hydroxyethyl)terephthalate (BHET), mono(2-hydroxyethyl)terephthalate (MHET), TPA and EG or their mixtures can be obtained (Mrigwani et al., 2022). TPA can then be purified and reused for PET manufacturing thus providing a route for a circular economy (Tournier et al., 2020). PET hydrolysis products can also be upcycled to commodity chemicals (Kim et al., 2019), polyhydroxyalkanoates (Kenny et al., 2008; Tiso et al., 2021), or even lycopene (Diao et al., 2023).

Research into the biological degradation of PET has revealed numerous bacterial and fungal strains harboring PET-degrading enzymes with over 8000 putative ortholog PETases identified in the genome databases (Gambarini et al., 2021). Highly efficient enzymes such as IsPETase from the bottle-dwelling bacterium *Ideonella sakaiensis* (Yoshida et al., 2016), or leaf-branch compost cutinase (LCC) identified through functional metagenomic screening (Sulaiman et al., 2012) have been reported to hydrolyze PET. Although biocatalytic processes are generally considered environmentally friendly, an in-depth life cycle assessment (LCA) of the enzymatic PET recycling revealed that it has up to 17 times worse environmental impact than manufacturing PET from virgin monomers (Uekert et al., 2022). To make biocatalytic and biotechnological processes truly advantageous further optimization work is needed.

The usefulness of PET oligomer degrading enzymes has been demonstrated in systems combining chemical and biological degradation, as well. PET degradation products obtained by glycolysis were efficiently converted to TPA by the addition of the Bs2Est esterase from *Bacillus subtilis* and subsequently transformed to catechol by an engineered *Escherichia coli* strain (Kim et al., 2021). Therefore, when searching for novel strains with PET degrading ability, it is important to search for enzymes that show high activity towards PET oligomers and other partial degradation products. This opens up the possibility of combining mechano- and green chemical depolymerizations with biocatalysis, as partially degraded polymers are still preferred substrates for enzymes and microorganisms.

In this study, an effort has been made to: (i) isolate and characterize a new bacterial strain capable of efficient degradation of BHET and other PET degradation intermediates, (ii) determine the enzymes responsible for this activity through genome analysis and expression of selected ones; (iii) and explore and evaluate how this strain can be utilized in biocatalytic degradation of multiple times extruded PET polymers mimicking the mechanical recycling process.

## 2. Materials and methods

### 2.1. Chemicals and reagents

Virgin polyethylene terephthalate (V-PET) resin in granulated form was purchased from Alpek Polyester UK Ltd. (Lazenby, UK). Components used to prepare media for bacterial growth were supplied by Acros Organics (Geel, Netherlands). Plastic monomers and polymers terephthalic acid (TPA), bis(2 hydroxyethyl) terephthalate (BHET), polycaprolactone diol (PCL) were purchased from Sigma Aldrich (Hamburg, Germany), Impranil DLN SD and Impranil DL 2077 from Covestro (Leverkusen, Germany). PET monomers and oligomers (1MER (1-(2-hydroxyethyl)-4-methylterephthalate), 1.5MER (ethylene glycol bis(methyl terephthalate)), 2MER (methyl bis(2-hydroxyethyl terephthalate)) and 3MER (methyl tris(2-hydroxyethyl terephthalate)) (Fig. S1) were previously synthesized and described (Djapovic et al., 2021). Analytical grades of sodium hydroxide (98%), ethylene glycol (99%) (EG), kanamycin, and other salts and solvents were obtained from Sigma Aldrich (Hamburg, Germany). Restriction enzymes and lysozyme were purchased from Promega (Madison, USA).

### 2.2. Isolation, identification, and morphology of strain BPM12

Strain BPM12 was isolated from soil with limited vegetation (Maganik, Montenegro, with coordinates: 42°43'54"N 19°17'02"E) using standard nutrient rich LB agar (Luria Bertani agar, 10 g/L tryptone, 5 g/L yeast extract, 10 g/L NaCl and 15 g/L agar) as a part of the effort to make a diverse in-house microbial collection. This collection was used for a variety of bioprospecting studies including plastic degradation. The growth of BPM12 was assessed and compared to *B. subtilis* 168 Marburg (MoBiTec, Goettingen, Germany) on MSF (Mannitol soy flower, 20 g/L soy flower, 20 g/L mannitol and 20 g/L agar), MSM (Minimal Salt Medium, 9 g/L Na<sub>2</sub>HPO<sub>4</sub> × 12H<sub>2</sub>O, 1.5 g/L KH<sub>2</sub>PO<sub>4</sub>, 1 g/L NH<sub>4</sub>Cl, 0.2 g/L MgSO<sub>4</sub> × 7H<sub>2</sub>O, 0.2 g/L CaCl<sub>2</sub> × 2H<sub>2</sub>O, 0.1% trace elements solution, 0.025% N-Z amine, 15 g/L agar and 20 g/L glucose as carbon source) and LB plates at 30 °C. Growth temperature (15–47 °C) and pH (pH 2–12, adjusted with HCl and NaOH) ranges were tested in LB broth. 1% of overnight culture in LB was used as inoculum and the growth was monitored by measuring the absorbance at 600 nm (Ultropec 3300pro, Amersham Biosciences, Amersham, UK) after 24 h of incubation in an orbital shaker at 180 rpm (MaxQ 6000, Thermo Fisher Scientific, Waltham, USA).

The ability to ferment different carbohydrate substrates was assessed using an API 50 CHB test kit (bioMérieux, Marcy l'Etoile, France) and hemolytic activity was tested using blood agar. For further identification of BPM12, 16S rDNA was amplified via PCR (FastGene TAQ PCR Kit, Nippon Genetics, Düren, Germany) using standard 1492R and 27F primers and sequenced by MacroGen Europe BV (Amsterdam, Netherlands). The strain was identified using BLAST (Basic Local Alignment Search Tool; <https://blast.ncbi.nlm.nih.gov/Blast.cgi>), while the sequences were analyzed, and the phylogenetic tree was constructed using Mega 7 program (Molecular Evolutionary Genetics Analysis; [www.megasoftware.net/home](http://www.megasoftware.net/home)) and Maximal likelihood method.

The morphology of the cells was assessed using fluorescent microscopy. An overnight culture of BPM12 from LB medium was collected by centrifugation (10 min at 5000 g, Eppendorf 5804 centrifuge, Hamburg, Germany), washed and resuspended using phosphate-buffered saline (PBS) (8 g/L NaCl, 0.2 g/L KCl, 1.44 g/L Na<sub>2</sub>HPO<sub>4</sub>, 0.24 g/L KH<sub>2</sub>PO<sub>4</sub>; pH 7.2). Cells were fixed with paraformaldehyde and stained with 10 µg/mL of Cl-TO-5 dye dissolved in PBS for 30 min at room temperature in the dark (Kurutos et al., 2020). The cells were visualized using an Olympus BX51 (Applied Imaging Corp., San Jose, USA) fluorescent microscope under 100000 × magnification.

### 2.3. Assessment of *B. subtilis* BPM12 plastic degrading potential

The plastic degrading potential of this bacterial strain was assessed using MSM agar plates supplemented with different plastic polymers and monomers as the sole carbon source applying previously described methodology (Molitor et al., 2020). The following substrates were used: TPA 10 g/L, BHET 10 g/L, PCL 6 g/L, Impranil DLN SD 6 g/L and Impranil DL-2077 9 g/L. The polymers and monomers were sonicated (Soniprep 150, MSE (UK) Ltd., Lindon, UK) for 10 min at 10 kHz before adding to the medium to obtain a stable suspension. The plates were incubated for 10 days at 30 °C and the formation of clearing zones was considered as a positive result.

#### 2.3.1. Biotransformation of PET-related model substrates

BHET and four PET-related model substrates (Djapovic et al., 2021) were used to further investigate the PET degrading potential of strain BPM12. Reactions were carried out in 3 mL of MSM medium with 1 mg/mL of PET-related model substrates (added from stock solutions of 30 mg/mL in methanol). Bacterial cells from fresh LB agar plates were scraped with inoculating loop and resuspended in MSM medium to make resting cells suspension of 20 mg wet weight per mL and 100 µL of the cell suspension was added to all reactions. Reactions were incubated for 5 days at 30 °C and 150 rpm (MaxQ 6000, Thermo Fisher Scientific, Waltham, USA).

To monitor the reaction progress, reaction products were extracted from 100 µL using ethyl acetate and analyzed using thin layer chromatography (TLC) on alumina plates with 0.25 mm silica layer (TCL Silica gel 60 F<sub>254</sub>, Sigma Aldrich (Hamburg, Germany)). The solvent system was chloroform/methanol (8:2) and visualized using UV light at 254 nm (Camag UV Lamp, Camag, Wilmington, USA).

### 2.3.2. High-performance liquid chromatography (HPLC) coupled with mass spectrometry (MS) analysis of biotransformation products

Samples were prepared by adding 1  $\mu$ L of 6 M HCl to 1 mL of the reaction aliquot, vortexed and centrifuged for 10 min at 12000 g (Eppendorf Centrifuge 5417 R, Hamburg, Germany). The supernatant was filtered through 0.2  $\mu$ m syringe filters. An UltiMate 3000 HPLC (Thermo Fisher Scientific, Waltham, USA) equipped with a Eurospher II 100-3 C18 A 150  $\times$  4.6 mm (Knauer, Berlin, Germany) column was used for HPLC analysis. The mobile phase consisted of 20% (v/v) acetonitrile and 80% (v/v) 2.5 mM sulfuric acid in ultrapure water at a flow rate of 0.8 mL/min under isocratic conditions. Detection of reaction products was carried out at 241 nm. The total run time was 25 min.

The exact masses of PET-related model substrate degradation products were confirmed using the same HPLC method (at a flow rate of 0.3 mL/min) and a TSQ Fortis™ Plus triple quadrupole mass spectrometer (Thermo Fisher Scientific, Waltham, USA) equipped with an H-ESI source in mixed scan mode and single ion monitoring (SIM) scan type. The ionization parameters were: 4500 V positive spray voltage, 2600 V negative spray voltage, 50 arbitrary units (arb) sheath gas flow rate, 10 arb aux gas flow rate, 325 °C ion transfer tube temperature and 350 °C vaporizer temperature.

### 2.4. BPM12 genome sequencing, annotation and analysis

A 350 bp insert size library was prepared and sequenced in paired-end mode (read length, 150 bp) by Novogene Europe on a NovaSeq 6000 (Illumina, San Diego, USA) instrument and a total of 4,607,303 paired reads were generated. Raw reads were preprocessed with TrimGalore v0.6.5 and cutadapt v2.9 (Martin, 2011). The Illumina adapter sequences were removed (with a stringency of 3), bases with a quality score less than 10 were trimmed and reads smaller than 100 bases or with no pair were discarded. *De novo* genome assembly was performed with Spades v3.13.0 (Bankevich et al., 2012). Genome completeness was assessed with BUSCO v5.1.2 using the Bacillales single-copy orthologs from OrthoDB v10 (Manni et al., 2021). Strain BPM12 was phylogenetically classified with the Genome Taxonomy Database Toolkit v2.0.0 (Chaumeil et al., 2020) against the GTDB release 207.

Gene prediction and functional annotation were performed with the NCBI Prokaryotic Genome Annotation Pipeline (PGAP, release 2022-10-03) (Li et al., 2021). Protein sequences were searched against the InterPro database with InterProScan v5.59-91.0 (Jones et al., 2014) and for signal peptides with SignalP v6.0 (Teufel et al., 2022). This Whole Genome Shotgun project has been deposited at DDBJ/ENA/GenBank under the accession .

The proteome of BPM12 was searched for homologs of biochemically characterized plastic-active enzymes from the PAZy database (Buchholz et al., 2021) with BLAST. The alignments were filtered for protein sequence identity > 40% and for > 70% alignment coverage of both the template and the target sequence. Next, the proteomes of 3 other *Bacillus* strains with reported activity on PET from RefSeq were gathered and clustered into homologous groups with the protein sequences of BPM12 using the Get\_Homologues software (Contreras-Moreira and Vinuesa, 2013) with the bidirectional BLAST best-hit option and default settings. The three *Bacillus* strains were: *Bacillus* sp. AIIW2, *B. albus* PFYN01 and *B. thuringiensis* C15 (accession numbers: GCF\_009932115.1, GCF\_004153665.1 and GCF\_004153515.1, respectively).

### 2.5. Overexpression and deletion of BPM12 carboxylesterase

BPM12 carboxylesterase (*bpm12CE* gene) was amplified via PCR (FastGene TAQ PCR Kit, Nippon Genetics, Düren, Germany) from BPM12 genomic DNA using BPM12CEF and BPM12CER primers containing the HindIII and BamHI restriction sites (Table S1). The amplicon was cloned into pGEM T-Easy (Promega, Madison, USA) vector, clones were confirmed via PCR amplification of the *Bpm12CE* gene and the appropriate restriction digest. The *bpm12CE* gene was then transferred to the pBE-S vector (Takara Bio, Shiga, Japan) using the HindIII and BamHI restriction enzymes. The pBE-S + *bpm12CE* plasmid constructs were used for the transformation of *B. subtilis* 168 Marburg (MoBiTec, Goettingen, Germany) cells and *B. subtilis* BPM12 using electroporation following the previously developed protocol (Yi and Kuipers, 2017). To create a *bpm12CE* knockout mutant a fusion gene consisting of two 1.5 kb flanking regions of *bpm12CE* and spectinomycin resistance gene was constructed using a set of primers shown in Table S1 and the NEBuilder HiFi DNA Assembly kit (New England Biolabs, Ipswich, USA). The fragment was used to transform *B. subtilis* BPM12 cells and *bpm12CE* was exchanged with the spectinomycin resistance gene. The knockout mutants were selected using spectinomycin 100  $\mu$ g/mL and were confirmed via PCR using appropriate primers.

Growth and clearance of BHET by recombinant strains was assessed on LB and MSM agar plates containing 5 g/L of BHET and kanamycin 50  $\mu$ g/mL or spectinomycin 100  $\mu$ g/mL and agar 15 g/L. Recombinant strains were also used in biotransformation reactions of BHET as described previously.

The esterase activity of the recombinant strains was tested using *p*-nitrophenyl butyrate (pNPB) as substrate (Jaeger and Kovacic, 2014). The assay reagent was prepared by dissolving 0.088 g/L pNPB in 20 mM Na-phosphate buffer (pH 7.2) with 0.17 g/L SDS and 10 g/L Triton-X-100. Protein preparations (50  $\mu$ L) were added to 150  $\mu$ L of the reagent and incubated for 5 min at 30 °C. The reaction was monitored at 410 nm (Epoch Microplate Spectrometer, BioTek, Winooski, USA). The protein concentration of samples was determined using Bicinchoninic Acid Kit for Protein Determination (Sigma Aldrich, Hamburg, Germany) and adjusted to 500  $\mu$ g/mL.



## 2.6. Interaction of BPM12 with PET materials

### 2.6.1. Preparation of multiple mechanically recycled PET films

V-PET pellets were dried for 6 h at 150 °C in a Universal Oven U (Memmert GmbH, Schwabach, Germany) under forced ventilation until moisture content was below 0.005%. Mechanical recycling of PET was simulated by means of hot melt extrusion (Fig. S2). A bench-top Prism™ twin-screw extruder (Thermo Electron GmbH, Karlsruhe, Germany) was used to produce the samples used in this study. The diameter of the screws used was 16 mm, with a 25/1 length-to-diameter ratio, at a screw speed of 50 rpm. A temperature profile of 70, 230, 250, 250 and 250 °C for the five temperature control zones, followed by a 3-roll calendar configuration used to form films. The virgin resin was extruded and reprocessed to produce the following materials: V-PET (0 recycling cycles), R<sup>2</sup>-PET (2 recycling cycles), and R<sub>5</sub>-PET (5 recycling cycles). Film samples were scissors cut into pieces (ca. 1 × 2 cm).

### 2.6.2. Characterization of virgin and multiple mechanically recycled PET films

Fourier Transform Infrared Spectroscopy (FTIR) was used to monitor chemical changes of extruded PET samples. Infrared spectra were obtained using a Perkin Elmer Spectrum One fitted with a universal attenuated total reflectance (ATR) sampling accessory (PerkinElmer, Waltham, USA), recorded over 16 scan cycles with a resolution of 4 cm<sup>-1</sup> in the spectral range of 4000–650 cm<sup>-1</sup> against air as background at room temperature (20 °C), at a resolution of 0.5 cm<sup>-1</sup> under a fixed universal compression force of 80 N. FTIR results were used to determine the ester carbonyl index (CI) that is a parameter used to investigate the degree of degradation of PET samples before and after chemical and biological treatments, as expressed in the following Eq. (1):

$$CI = \text{Band intensity at } 1713 \text{ cm}^{-1} / \text{Band intensity at } 1408 \text{ cm}^{-1} \quad (1)$$

The thermal behavior of extruded PET samples was studied by Differential Scanning Calorimetry (DSC) recorded on a 2920 Modulated DSC (TA Instruments, New Castle, USA), previously calibrated with indium standard. Samples of 6 to 9 mg were weighted on an Explorer EX124 analytical balance (OHAUS Corporation, Parsippany, USA). Thermal analysis was conducted from 30 °C to 275 °C at a heating rate of 10 °C/min using nitrogen as purge gas at a flow rate of 30 mL/min. The crystallinity index ( $X_c$ ) was calculated from the second heating cycle as follows (Eq. (2)):

$$X_c (\%) = ((\Delta H_m - \Delta H_c) / \Delta H_m^\circ) \times 100 \quad (2)$$

where,  $\Delta H_m$  is the apparent melt enthalpy of the specimen tested,  $\Delta H_c$  is the heat of cold crystallization, and  $\Delta H_m^\circ$  is a reference value that represents the heat of melting if the PET were 100% crystalline (140 J/g) (Wunderlich, 1973).

Scanning electron microscopy (SEM) images were obtained using Mira XMU SEM (Tescan™, Brno, Czech Republic) in backscattered electron mode for surface analysis. The accelerating voltage used was 10 kV. Prior to analysis, tested samples were placed on an aluminum stub and sputtered with a thin layer of gold using a Baltec SCD 005 sputter coater (New York, United States) for 110 s at 0.1 mbar vacuum.

### 2.6.3. Chemical recycling of virgin and recycled PET via microwave (MW) assisted hydrolysis

The efficiency of MW-assisted hydrolytic depolymerization of PET was evaluated following previously published work with slight modification (Azeem et al., 2022). Typically, V-PET, R<sub>2</sub>-PET and R<sub>5</sub>-PET films were separately mixed in 10% (w/v) sodium carbonate (Na<sub>2</sub>CO<sub>3</sub>) dissolved in 1 mL of EG. The sample suspensions were then MW irradiated at 350 W in a domestic microwave (MW) oven (Wavedom, LG, Seoul, South Korea) for 1.5 min. Dissolved PET was precipitated by the addition of distilled water. Finally, the obtained mixture was filtered, and the filtrate containing soluble monomers was analyzed by HPLC. The residual PET samples were dried overnight at 70 °C and kept in sealed bags for FTIR and DSC analysis. The depolymerization of PET was calculated using the following Eq. (3):

$$\text{PET Conversion (\%)} = \left(1 - \frac{\text{Weight of residual PET}}{\text{Weight of initial PET}}\right) \times 100 \quad (3)$$

The selectivity of soluble monomers was quantified from the HPLC chromatograms and the yield of TPA was calculated using Eq. (4):

$$\text{Yield of TPA(\%)} = \frac{(\text{Conversion of PET (\%)} \times \text{Selectivity of TPA (\%)})}{100} \quad (4)$$

The TPA monomer was then precipitated by the addition of 2 mL of concentrated HCl (34%, v/v) to the cooled filtrate. The separated TPA from each sample was washed with water, dried overnight at 70 °C and characterized by FTIR against TPA commercial standard.

## 2.7. Biodegradation of PET materials

### 2.7.1. *B. subtilis* BPM12 attachment to PET films

The attachment of *B. subtilis* BPM12 to PET films was assessed using the protocol reported by Ferrero et al. (2022). Briefly, an overnight culture of *B. subtilis* BPM12 (0.1%, v/v) was used to inoculate LB medium containing pieces of PET

films (rinsed with EtOH (70%, v/v) and dried under laminar flow). After 7 days of incubation at 30 °C the films were rinsed with water and stained with crystal violet solution (1 g/L) for 20 min. The films were then destained using 30% (v/v) acetic acid and the measured absorbance (Epoch Microplate Spectrometer, BioTek, Winooski, USA) at 550 nm of the remaining solution was used as an indicator of cell attachment.

### 2.7.2. Biodegradation of PET films using whole cells

PET biodegradation experiments were performed in flasks with 25 mL of MSM medium containing glucose (20 g/L) as a carbon source. PET strips (cut into pieces of approximately 0.5 cm × 2.5 cm, rinsed with 70% (v/v) EtOH, dried under laminar flow and weighed) were added to flasks. The flasks were then inoculated with 1% (v/v) overnight culture of *B. subtilis* BPM12 (grown in MSM medium) and incubated at 30 °C, 180 rpm (MaxQ 6000, Thermo Fisher Scientific, Waltham, USA). Appropriate controls, without the addition of bacterial inoculum were also included. After 4 and 8 weeks, PET strips were taken out, washed with EtOH (70%, v/v), air dried and weighed and the medium supernatant was analyzed via HPLC.

### 2.7.3. Biodegradation of PET films using total protein preparations

Strain BPM12 was grown in LB supplemented with BHET (2 g/L) at 30 °C, 180 rpm until OD<sub>600</sub> reached 5–6. The culture was centrifuged for 10 min at 5000 × g (Eppendorf centrifuge 5804, Hamburg, Germany) and the supernatant was stored at 4 °C until use. The cell pellet was resuspended in sodium phosphate buffer (20 mM, pH 7.2) supplemented with lysozyme, and incubated for 30 min at 37 °C, followed by sonication of 4 pulses of 15 s at 20 kHz (Soniprep 150, MSE (UK) Ltd., London, UK). The suspension was clarified by centrifugation for 30 min at 20000 × g, 4 °C (Eppendorf Centrifuge 5417 R, Hamburg, Germany) to obtain the cell-free extract. The total protein mixture was prepared by mixing cell-free extract and culture supernatant in equal volumes. The protein concentration of samples was determined using Bicinchoninic Acid Kit for Protein Determination (Sigma Aldrich, Hamburg, Germany) and adjusted to 500 µg/mL. Total protein preparations were stored at –20 °C until use.

Enzymatic biodegradation of recycled PET plastic films was performed in sodium phosphate buffer (20 mM, pH 7.2) using total protein mixture from strain BPM12. The experiments were performed in glass flasks, in 7 mL buffer volume, at 30 °C, 180 rpm, for 4 and 8 weeks. Aliquots (1 mL) of total protein preparations were added every week, while aliquots (1 mL) of tested samples were taken and stored at –20 °C for further HPLC analysis. The same procedure was applied to controls – PET plastic films in sodium phosphate buffer, which was also exchanged weekly.

After biodegradation experiments, PET plastic films were washed with EtOH (70%, v/v), air dried and weighed. All samples were analyzed via SEM analysis as previously described for characterization of virgin and multiple mechanically recycled PET films.

## 2.8. Statistical analysis

The results are presented as mean ± standard deviation (SD). Statistical analysis was done by comparing means using *t*-test (Two-Sample Assuming Equal Variances) and one-way ANalysis Of VAriance (ANOVA, Single Factor), with Fisher's Least Significant Difference (LSD) post-hoc test. The level of statistical significance is expressed as a *p*-value (probability value), and *p* ≤ 0.05 was considered statistically significant. Statistical analysis tests were performed in Microsoft Excel Spreadsheet Software by Data Analysis Tools add-in.

## 3. Results and discussion

### 3.1. Isolation and identification of *Bacillus* sp. BPM12

BPM12 is a mesophilic bacterium isolated from the pristine soil sample from the mountain slope with limited vegetation. During the phenotypic screening, it was distinguished by its ability to efficiently grow on BHET, PCL and Impranil DL 2077 as a sole carbon sources, using MSM medium. Clearing halos on BHET plates were observed after three days of incubation at 30 °C, suggesting BPM12 a potentially useful strain for PET and other plastics degradation (Fig. 1a). The strain could grow at temperatures from 20 to 47 °C and at pH values from 6 to 10. It fermented 26 out of the 49 carbohydrates, including simple sugars such as mannose, fructose, and glucose but also polysaccharides such as starch and glycogen (Table S2). It was not able to grow on TPA as the sole carbon source. The 16S rRNA gene sequence placed BPM12 within the *Bacillus* genus most closely related to *B. subtilis* strain BAB-1684 (Accession number: KF535143.1) with 99% sequence identity (Fig. 1b). The strain was named *Bacillus* sp. BPM12 and the 16S sequence was deposited to GenBank under the accession number OQ381249.

BPM12 grew equally well on minimal and nutrient rich solid media within 24 h of inoculation. It formed creamy-white and orange colonies with smooth irregular edges on MSM and MSF, respectively. Colonies on LB plates were opaque and circular. The growth of *Bacillus* sp. BPM12 was also compared to *B. subtilis* 168 on different media (Fig. S3a). Neither strain exhibited hemolytic activity. Fluorescent microscopy revealed BPM12 cells were rod-shaped with an approximate size of 0.8–1.0 × 5–7 µm which is consistent with *Bacillus* spp. morphology (Fig. S3b).

*Bacillus* is a remarkably diverse bacterial genera, able to grow within ecologically diverse environments (Earl et al., 2008). *Bacillus* strains have been investigated for xenobiotic degradation such as the degradation of pesticides cypermethrin, imidacloprid, fipronil, and sulfosulfuron reaching degradation rates of up to 99% (Gangola et al., 2021, 2022).

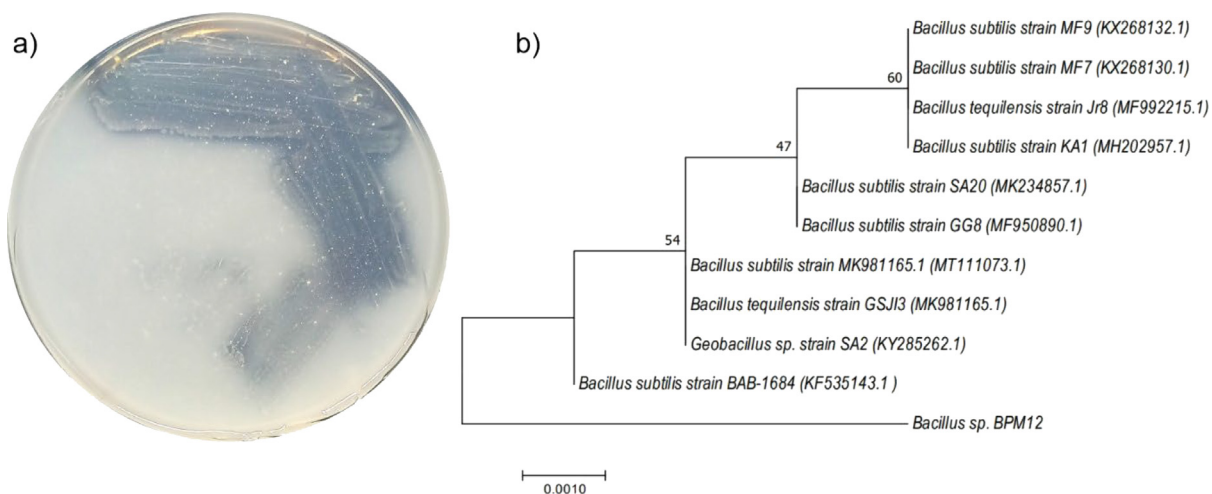


**Fig. 1.** (a) *Bacillus sp.* BPM12 forming clearing zones on MSM agar plate with BHET as the sole source of carbon and energy after 3 days at 30 °C; (b) Maximum likelihood tree showing the relationship of *Bacillus sp.* BPM12 to 10 of the most closely related strains. Bootstrap values based on 1000 replications are displayed on the nodes of the tree. The scale bar represents genetic distance.

Members of the *Bacillus* genus have been reported to degrade various plastic polymers including PET (Ribitsch et al., 2011), polyurethanes (Shah et al., 2013) and polylactic acid (Bonifer et al., 2019) and have been identified in several consortiums capable of degrading recalcitrant plastics (Roberts et al., 2020; Shah et al., 2016; Skariyachan et al., 2017). *Bacillus sp.* BPM12 growth profile at temperatures above 40 °C as well as tolerance towards alkaline conditions matches that of some previously reported *Bacillus* strains (Ali et al., 2016; Hanim, 2017; Wang et al., 2019) and is highly desirable for biotechnological applications where biocatalysts need to withstand harsh conditions. Another valuable trait of *B. subtilis* is the ability to form highly resistant endospores in response to nutrient deprivation and other environmental stresses, which had already been used for efficient surface display of relevant enzymes including PETases (Jia et al., 2022). Therefore, *Bacillus sp.* BPM12 was further investigated as a potential biocatalyst for PET degradation.

### 3.2. Degradation of PET-related model substrates

Resting whole cells of *Bacillus sp.* BPM12 were able to hydrolyze BHET, 1MER and 2MER, while 1.5MER and 3MER showed only traces of degradation products, based on HPLC and TLC analysis (Fig. 2; Figs. S4–S6). During the course of the reaction, 1000 mg/L of BHET was completely converted to MHET and TPA within 120 h at 30 °C (Fig. 2a). The ratio of TPA to MHET was 1:6 within this time period. The control reactions showed some BHET auto-hydrolysis to MHET ( $\leq 5\%$ , w/w). These results suggest that BHET is firstly converted to MHET that is subsequently converted to TPA at a considerably slower rate, a trend also observed among different PET degrading enzymes (Mrigwani et al., 2022). *Bacillus sp.* BPM12 is more efficient in BHET conversion when compared to *Enterobacter sp.* HY1, which was able to degrade 80.8% of BHET (1000 mg/L) in 120 h at 30 °C (Qiu et al., 2020), and comparable to a *Yarrowia lipolytica* wild-type (Wt) strain which could convert 500 mg/L of BHET in about 48 h at 29 °C (da Costa et al., 2020). However, engineered strains expressing IsPETase achieve much higher conversion rates, reaching up to 5 g/L and 2 g/L when the enzyme is expressed in *Y. lipolytica* Po1fP and in *B. subtilis*, respectively (Qi et al., 2021).

1MER of PET was also found to be fully converted to mono-methyl terephthalate (MTPA), MHET and TPA, suggesting that *Bacillus sp.* BPM12 can cleave both ester bonds of 1MER (Fig. 2b). Given that the main product detected was MTPA, when 1MER was used as a substrate, the preferred cleavage site was at the ethyl moiety. The slow conversion of MHET and MTPA to TPA by *Bacillus sp.* BPM12 may be due to MHET inhibition as it has been shown that MHET considerably inhibited the hydrolytic activity of Bs2Est (Kim et al., 2021). 1.5MER and 2MER were converted to MTPA, MHET and TPA confirming both exo- and endo-cleaving activity of *Bacillus sp.* BPM12 (Figs. S4 and S5). 2MER is most likely firstly converted to MTPA and BHET via endo-cleaving activity and then further broken down to MHET and TPA via exo-cleaving activity, a mechanism previously shown when Bs2Est was used as a biocatalyst (Kim et al., 2021). 3MER was found to be much harder to degrade with only traces of degradation products detected, which can be contributed to the poor solubility and high hydrophobicity of this substrate (Fig. S6). Similarly, recently described polyesterase from *Moraxella sp.* (MoPE) capable of degrading highly crystalline PET was characterized using the same set of substrates revealing the same mode of action (Nikolaivits et al., 2022).

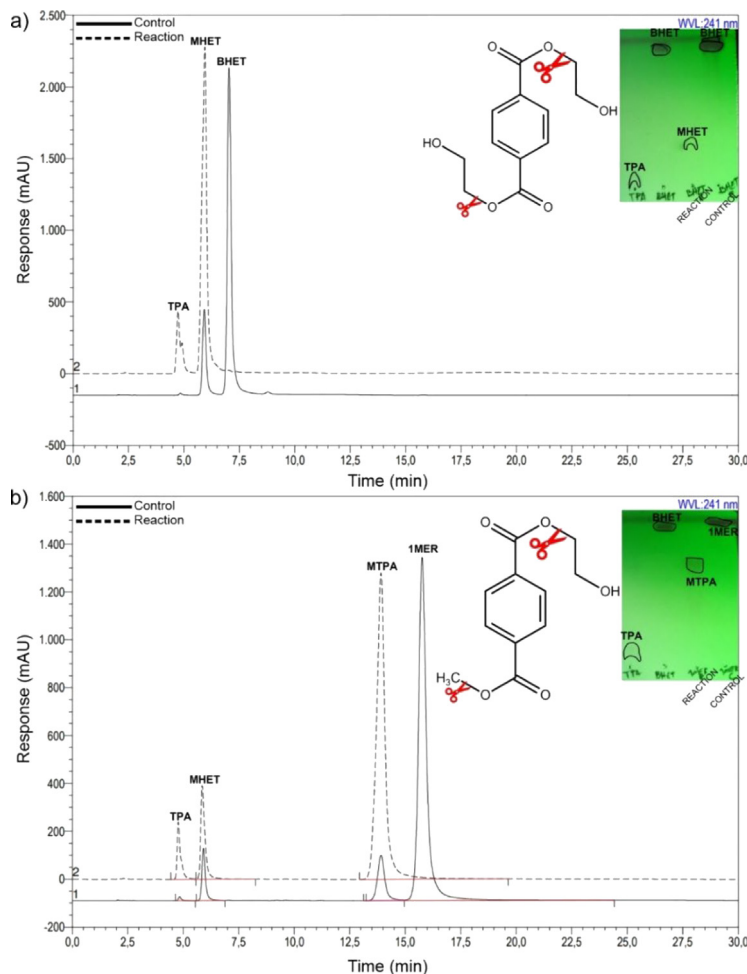


**Fig. 2.** BHET and 1MER biotransformation using whole cells of *Bacillus* sp. BPM12 was monitored via HPLC and TLC. (a) BPM12 resting cells transformation of BHET; (b) BPM12 resting cells transformation of 1MER of PET. In the HPLC chromatograms, the full lines represent the control reactions (no biocatalyst), while the dashed lines represent the reactions containing BPM12 cells.

### 3.3. *Bacillus* sp. BPM12 genome analysis

The genome assembly consisted of 137 contigs, is 4160070 bp long and is 98.6% complete based on BUSCO (Benchmarking Universal Single-Copy Orthologs) analysis. Strain BPM12 was confirmed to be *B. subtilis* sp. with the Genome Taxonomy Database Toolkit. The predicted proteome of BPM12 consists of 4196 proteins and 3406 of them were clustered in 3301 homologous groups with proteins from the other three *Bacillus* strains with reported activity on PET polymer. Almost half of the total BPM12 proteins are core proteins with homologs in all considered genomes and most BPM12 proteins were clustered with proteins of the AIIW2 strain with which it shares 78.2% whole-genome average nucleotide identity (Fig. 3).

*Bacillus* sp. AIIW2 is a marine isolate that was found to utilize PET as a carbon source (Kumari et al., 2021). *B. thuringiensis* C15 and *B. albus* PFYN01 are members of a 5 strain consortium that grew synergistically in the presence of PET as the sole carbon source (Roberts et al., 2020). Both strains tested negative for lipase activity with C15 being unable to grow on PET in the absence of the rest of the consortium.

The proteome of BPM12 contains 5 enzymes that share high similarity with known plastic-active enzymes from PAZY (Table 1). These 5 enzymes include three esterases and two serine proteases. The two serine proteases are core genes with homologs in all considered genomes. The CE WP\_216995529.1 is almost 100% identical to the intracellular PETase from *B. subtilis* strain 4P3-11 that can hydrolyze 3PET and PET films (Ribitsch et al., 2011) and has no homologs in the other three proteomes. No significant homology was detected with known MHET-ases such as Mle046 (Meyer-Cifuentes and Öztürk, 2021). The lipase LipA and the esterase EstB are both secreted and are members of the same InterPro family (IPR002918). They form a homologous cluster with an alpha/beta hydrolase from isolate AIIW2 that lacks a signal peptide. Kumari et al. report a non-secreted CE (accession number: WP\_020451834.1) displaying the highest relative fold change in the



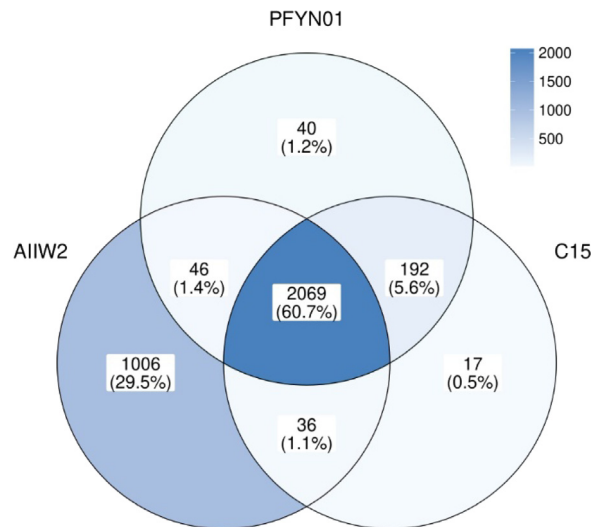


**Fig. 3.** *B. subtilis* BPM12 proteins clustered in homologous groups with proteins from known PET-active *Bacillus* strains (*B. albus* PFYN01, *Bacillus* sp. AllW2, and *B. thuringiensis* C15).

**Table 1**

*B. subtilis* BPM12 proteins and their PAZy homologs.

BPM12	PAZy	Identity %	Active on
Carboxylesterase (WP_216995529.1)	PETase (ADH43200.1)	98.9	PET
Subtilisin AprE (WP_015715621.1)	<i>Subtilisin carlsberg</i> (P00780)	65.2	PLA
Lipase LipA (WP_086343408.1)	PLaA (Q83VD0)	48.8	PLA
Esterase EstB (WP_003243184.1)	PLaA (Q83VD0)	46.1	PLA
Serine protease Isp (WP_029946400.1)	Subtilisin savinase (P29599.1)	45.4	PLA

presence of PET based on quantitative reverse transcriptase–polymerase chain reaction analysis (Kumari et al., 2021). This CE clustered with the alpha/beta hydrolase WP\_014480039.1 of BPM12. The two enzymes share 68% sequence identity and have the same length.

The genome of BPM12 was further searched for enzymes with esterase activity, the main activity associated with PET degradation but involved in pesticide degradation as well (Gangola et al., 2018), based on the functional protein domains identified with InterProScan. This analysis identified 63 esterases with 7 of them being predicted to be secreted. Only one of the secreted esterases, the phosphodiesterase WP\_264240018.1, is a core gene present in all considered genomes. The GDSL esterase WP\_264240216.1 has no homologs in any other isolate and the remaining 5 secreted esterases, including LipA and estB, have homologs only in the AllW2 genome. Recently, pangenomic analysis that included 88 *Bacillus* species, revealed many other biodegradation genes involved in plastics and plasticizers degradation through the Plastic Microbial Biodegradation Database (PMBD) apart from the genes implicated in PET degradation (Edwards et al., 2022). An esterase from *B. subtilis* was immobilized on halloysite nanotubes and completely degraded dibutyl phthalate (Balci et al., 2023). Furthermore, *Bacillus* species were also shown to produce a number of valuable proteases and enzymes involved in metal tolerance and removal (Liya et al., 2023; Sharma et al., 2022).

### 3.4. Expression of BPM12CE

Given the high sequence identity of BPM12CE (Table S3) to a known PETase from *B. subtilis* (WP\_216995529.1), BPM12CE was selected as the most likely gene responsible for the PET-related substrate degradation activity. Therefore, the gene was deleted from the genome of *B. subtilis* BPM12 to create a knockout mutant. The deletion of *Bpm12CE* indeed led to the almost complete loss of BHET degrading activity (Fig. S7a) with only a faint clearing halo visible, as well as the loss of ability to grow on BHET as the sole carbon source, corroborating the hypothesis that *B. subtilis* BPM12 utilizes EG during growth on BHET.

To further investigate its BHET degrading activity *bpm12CE* gene was cloned into a *Bacillus* expression vector and introduced into both *B. subtilis* BPM12 and 168. The general esterase activity using pNPB was detected in both strains and in both intracellular and extracellular protein fractions (Fig. S8). The relative intracellular esterase activity was generally lower in comparison to extracellular protein fractions (between 1.4- and 5.9-fold) but remained comparable between the strains. Nevertheless, the extracellular esterase activity of recombinant strains increased by 1.8- and 3.2- fold in *B. subtilis* BPM12 and *B. subtilis* 168, respectively, compared to Wt strains. To get a better insight into specific BHETase

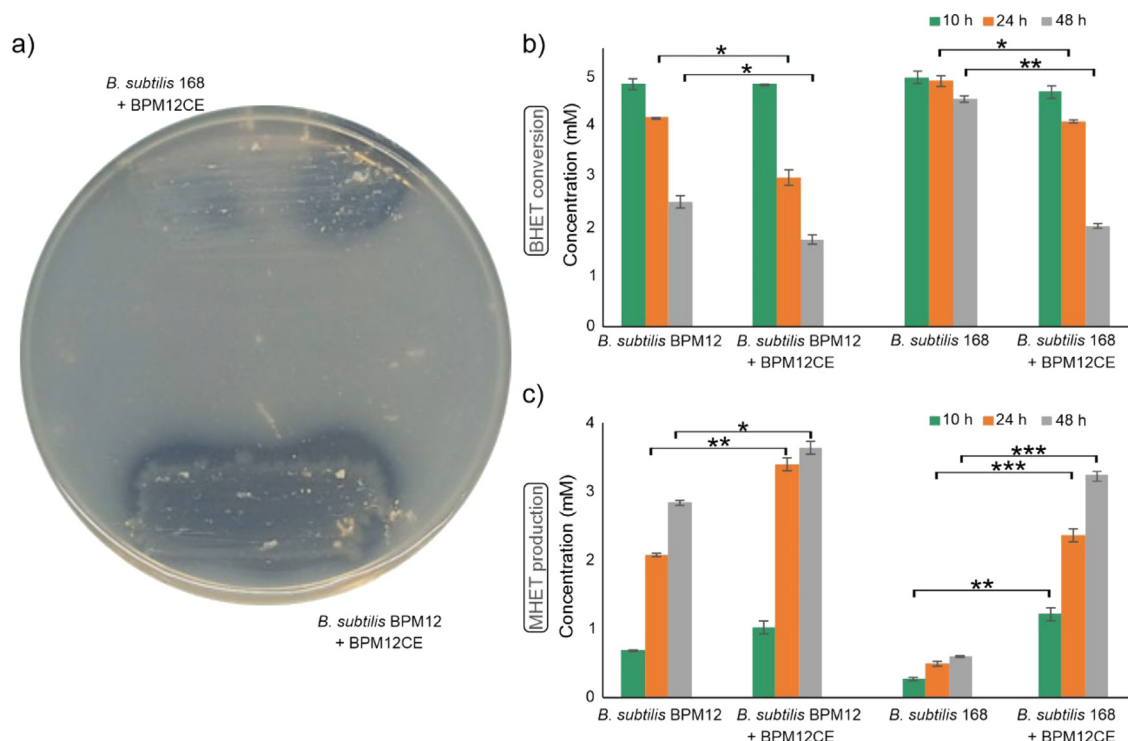


**Fig. 4.** Growth and activity of BPM12 Wt and *B. subtilis* 168 strains expressing BPM12CE. (a) MSM agar plates with BHET as the sole carbon source after 10 h, 24 h and 48 h at 30 °C; (b) BHET conversion in liquid culture; (c) MHET production in liquid culture after 10 h, 24 h and 48 h incubation. Results were analyzed using ANOVA test and post-hoc Fisher's LSD test (\*  $p \leq 0.05$ , \*\*  $p \leq 0.01$ , \*\*\*  $p \leq 0.001$ ).

activity, the recombinant strains were tested using BHET as a substrate on plates and in liquid biotransformation reactions using whole cells (Fig. 4). Initially, *B. subtilis* 168 did not form clearing halos on BHET-containing plates while BPM12 did (Fig. 1, Fig. S7b). When transformed, both strains exhibited BHET degrading activity, however, recombinant *B. subtilis* BPM12 was able to grow better and form larger zones of clearance on MSM agar containing BHET as a sole carbon source (Fig. 4a). In liquid culture, BHET degradation by *B. subtilis* 168 harboring BPM12CE showed a 6-fold increase in comparison to untransformed *B. subtilis* 168 (Fig. 4b), clearly demonstrating that BPM12CE was indeed responsible for BHET conversion. Furthermore, the activity of recombinant *B. subtilis* 168 was almost identical to that of *B. subtilis* BPM12 Wt strain. Homologous expression of BPM12CE in *B. subtilis* BPM12 led to 1.6-fold increase in the MHET production within the first 24 h in comparison to the Wt strain (Fig. 4c).

*Bacillus* is a more favorable expression system in comparison to *E. coli* due to intrinsic secretion capacity and better protein folding resulting in a higher yield of more stable enzymes (Souza et al., 2021; Wei et al., 2019). Four enzymes with PETase activity have been successfully expressed in *Bacillus* species so far. *T. fusca* hydrolase (TfH) was obtained using *B. megaterium* with an excellent yield of 240  $\mu\text{g/L}$  at a 2 L scale (Yang et al., 2007). Subsequently, a highly similar enzyme TfCut2 was also obtained from *B. subtilis* with higher purity and its activity on PET materials was demonstrated. It was shown that TfCut2 is more thermostable when expressed in *Bacillus* compared to *E. coli* with a 4 °C higher melting point (Wei et al., 2019). Signal peptide optimization allowed for the enhanced secretion of IsPETase (Huang et al., 2018; Wang et al., 2020) and BhrPETase (Xi et al., 2021). Given that *B. subtilis* BPM12 possesses intrinsic activity towards PET-related substrates it could serve as an ideal platform for the expression of various PETases and other auxiliary enzymes to increase polymer degrading capacity.

### 3.5. Preparation, characterization and chemical recycling of PET materials

Mechanical recycling has been the most common method used to recover PET and other recyclable plastics because it is relatively easy and economical (Faraca et al., 2019). Nevertheless, the cleavage of the long polymer chains caused by thermomechanical degradation is a common problem that affects the properties of mechanically recycled PET during reprocessing and lifetime (Makkam and Harnnarongchai, 2014). The resulting shorter polymer chains are expected to be more susceptible to biodegradation, which succeeds abiotic degradation (Mohanani et al., 2020).

The properties of the virgin and recycled PET materials obtained from the chemical and thermal analysis are shown in Table 2. Chemical analysis by FTIR accessed possible chemical changes due to thermomechanical degradation of PET chains

**Table 2**

Properties of the untreated virgin and recycled PET films and their respective residues obtained from post MW-assisted depolymerization treatment.

Sample	Untreated			MW-assisted treatment		
	$T_m$ (°C) <sup>a</sup>	$X_c$ <sup>b</sup>	CI <sup>c</sup>	$T_m$ (°C) <sup>a</sup>	$X_c$ <sup>b</sup>	CI <sup>c</sup>
V-PET	246.1	34.9	4.8	246.8	19.5	0.6
R <sub>2</sub> -PET	249.0	38.6	4.4	232.3	24.8	3.2
R <sub>5</sub> -PET	250.2	44.5	4.2	220.9	11.1	1.4

<sup>a</sup>Melting temperature;

<sup>b</sup>Crystallinity index;

<sup>c</sup>Carbonyl index.

over the reprocessing cycles (Holland and Hay, 2002). The IR spectra of virgin and recycled PET samples are shown in the 1900–650  $\text{cm}^{-1}$  range (Fig. S9). The band at 1570  $\text{cm}^{-1}$  is related to a conjugated aromatic structure in the PET samples, while the region from 950 to 750  $\text{cm}^{-1}$  is attributed to C–H deformation. On one hand, no significant changes in the aforementioned bands were observed for both R<sub>2</sub>-PET and R<sub>5</sub>-PET in comparison to the IR spectrum of V-PET, suggesting no clear sign of thermal degradation resulting from the extrusion process. Accordingly, it can be seen from Table 2 that the mechanical recycling process had no significant impact on the CI for the studied wavenumber that rather decreased slightly from 4.84 in the V-PET to 4.42 and 4.18 in the R<sub>2</sub>-PET and R<sub>5</sub>-PET materials, respectively. On the other hand, there were clear changes in the intensity of the bands at 1470, 1370 and 1340  $\text{cm}^{-1}$  assigned to CH<sub>2</sub> bending and wagging modes of trans conformers, which have been associated with the degree of crystallinity of the PET materials (Sammon et al., 2000). This is evidenced by a subsequent increase in both the glass transition temperature ( $T_g$ ) and crystallinity index ( $X_c$ ) calculated from the second heating step of the DSC thermograms of reprocessed R<sub>2</sub>-PET and R<sub>5</sub>-PET materials when compared to the values obtained for V-PET (Fig. S10). In particular, the role of the crystalline phase in the performance of recycled PET has been investigated elsewhere (Badia et al., 2012). Therefore, the increase of the  $X_c$  observed herein ranging from 34.99 in the V-PET to 44.48 in the R<sub>5</sub>-PET material was attributed to the growth of more crystalline domains promoted by the formation of shorter polymer fragments that resulted from the cleavage of the polymer backbone, and possibly act as nuclei upon crystallization.

V-PET, R<sub>2</sub>-PET and R<sub>5</sub>-PET underwent chemical recycling via MW-assisted hydrolysis. The residual PET obtained was weighed and the conversion of PET (%) was calculated. The reaction products dissolved in the cooled filtrate were analyzed by HPLC. The effects of different PET pretreatment on the conversion of PET, the selectivity of soluble monomers and the yield of TPA are illustrated in Fig. S11. It was observed that the rate of conversion was only 75.4% when applying MW-assisted hydrolysis reaction on untreated virgin PET and then increased to 86.9 and 94.2% when hydrolyzing R<sub>2</sub>-PET and R<sub>5</sub>-PET, respectively. Such a significant increase in depolymerization efficiency with the mechanically recycled PET at only 1.5 min MW irradiation time could be attributed to the modifications that took place in the properties of the virgin PET after several cycles of mechanical recycling. The yield of TPA increased from 36.5% for the virgin PET sample to 38.1% and 56.1% for R<sub>2</sub>-PET and R<sub>5</sub>-PET, respectively (Fig. S11). Noticeably, the selectivity of MHET was much higher than that of BHET for all samples. It was also observed that the selectivity of BHET and MHET were almost the same for all chemically treated samples indicating that modifications that occurred by the pretreatment process did not have a significant effect on the selectivity of depolymerization products obtained post chemical recycling. Moreover, the residual PET obtained post chemical recycling process for the studied PET samples showed a decrease in the crystallinity and carbonyl index from the original samples as demonstrated in Table 2. The  $X_c$  of the obtained residues ranged between 11 and 25 while the carbonyl index ranged between 0.6 and 3.2. It is also worth mentioning that the DSC results of the obtained residues post chemical recycling process, especially R<sub>2</sub>-PET and R<sub>5</sub>-PET, have shown a decrease in the melting point temperatures in comparison to the original samples. This could be attributed to the production of lower molecular weight PET oligomers after the chemical recycling process exhibiting a melting endotherm peaking at temperatures lower than that of untreated PET (Chaudhary et al., 2013). The identity of the TPA white powder monomer precipitated post the MW-assisted hydrolysis process was confirmed using FTIR analysis (Fig. S12). FTIR spectra of precipitated TPA from all treated PET samples were almost identical to standard TPA and TPA reported in the literature (Azeem et al., 2022).

### 3.6. Degradation of PET material samples by *B. subtilis* BPM12 whole-cells and total protein extracts

As previously reported, biofilm formation is an important factor contributing to the initiation of plastic degradation (Maheswaran et al., 2023), therefore the ability of *B. subtilis* BPM12 to attach to PET films was assessed. *B. subtilis* BPM12 showed the ability to form biofilms on both, virgin and recycled PET films (Fig. 5a).

The recycling process apparently increased the ability of cell attachment to the films, possibly due to changes on the surface of the films. However, whole-cell degradation of PET materials using *B. subtilis* BPM12 did not lead to any detectable weight changes after 8 weeks of incubation, while weight changes after enzymatic biodegradation of virgin and recycled PET films are represented in Table S4. Although the weight loss of PET materials was minimal and comparable amongst samples, HPLC analysis revealed the release of PET degradation products, mostly TPA and MHET when cell-free

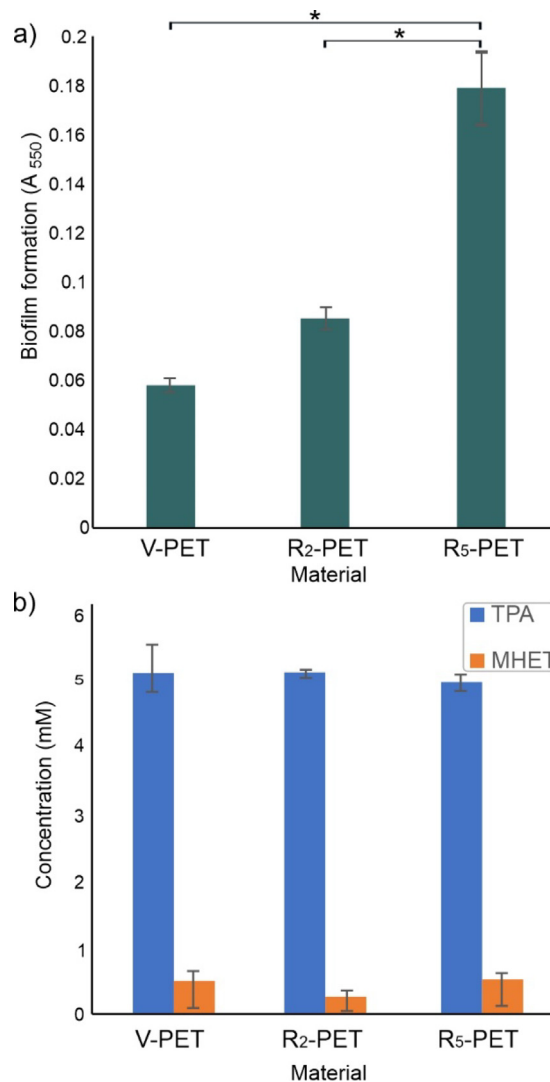


**Fig. 5.** *B. subtilis* BPM12 attachment on PET materials (a) and biodegradation products (TPA and MHET) detected after 8 weeks (b) of incubation of PET materials with total protein preparation at 30 °C. Results were analyzed using ANOVA test and post-hoc Fisher's LSD test,  $p \leq 0.05$  was considered statistically significant.

enzymes from this strain were incubated with materials over this time period (Fig. 5b). Although the initial attachment of the whole cells was 2-fold higher in the case of re-extruded materials, the yield of degradation products using enzymes from this strain was comparable for all used materials. As in the case of PET MW-assisted hydrolysis, material properties after enzymatic treatment were assessed (Table 3). Indeed, enzymatic treatment did not have a significant effect on the materials'  $T_m$  or  $CI$ . However, the  $X_c$  for R5-PET has increased by 40% in comparison to that of the untreated R5-PET material (Table 2), which further implies that enzymatic activity was focused on amorphous regions of the material.

These results were further confirmed by SEM analysis of non-treated and enzymatically treated materials. As presented in Fig. 6, the surface of non-treated virgin PET is smooth, with few abrasions, while in the case of recycled (re-extruded) PET, multiple surface plications were detected, which explains biofilm formation susceptibility of these samples (Perera-Costa et al., 2014). Furthermore, a clear difference between treated and control samples has been observed. Surface modifications in the form of cracks and dents could be a result of degradation of the preferred amorphous regions in the materials while crystalline structures have remained intact.

The preference of PET-degrading enzymes towards amorphous regions has been discussed in various studies (Kawai et al., 2019; Tournier et al., 2020), however further analysis is required in order to determine the exact fractions composition of the samples (rigid amorphous fraction, mobile amorphous fraction, crystallinity degree). Changes on the surface of examined materials imply that enzymatic treatment has led to materials surface erosion which is in accordance with the biodegradation product release detected (Fig. 5b).



**Table 3**  
Properties of the virgin and recycled PET residues obtained post BPM12 enzymatic treatment.

Sample	$T_m$ ( $^{\circ}\text{C}$ ) <sup>a</sup>	$X_c$ <sup>b</sup>	CI <sup>c</sup>
V-PET	246.1	34.9	4.9
R <sub>2</sub> -PET	249.0	38.6	4.3
R <sub>5</sub> -PET	250.0	62.3	4.2

<sup>a</sup>Melting temperature;

<sup>b</sup>Crystallinity index;

<sup>c</sup>Carbonyl index.

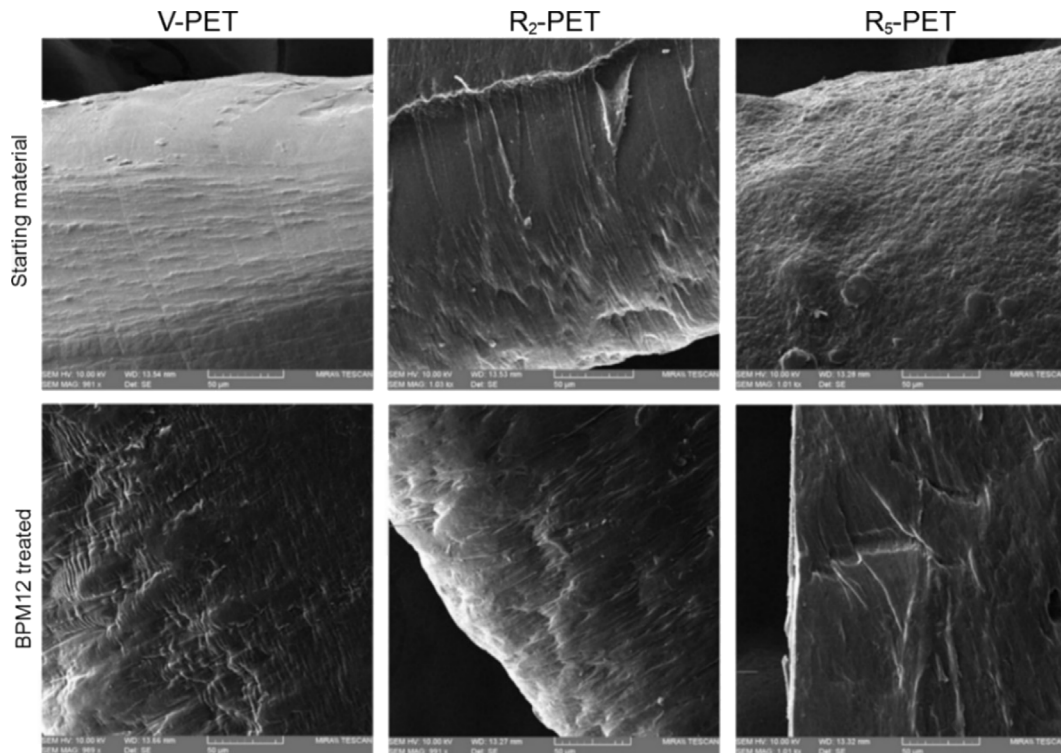


**Fig. 6.** SEM images of V-PET, R<sub>2</sub>-PET, and R<sub>5</sub>-PET films before and after the exposure to BPM12 biodegradation for 8 weeks (1000 × magnification, scale bar = 50 µm).

Additionally, erosion degree appears to correlate with BHET and MHET release. Similar surface modifications have been previously reported by Chen et al. in a study where the whole-cell biocatalyst was engineered to improve degradation of highly crystalline PET materials (crystallinity over 45%) (Chen et al., 2022). After the exposure of materials to BPM12, virgin PET (sample with the lowest crystallinity percentage) has shown the most significant surface modification correspondingly with the study by Thomsen et al. where it was shown that PET degradation is directly correlated to crystallinity percentage (Thomsen et al., 2022).

Taken together, polymeric PET both mechanically recycled and virgin, is not a suitable substrate for microbial or enzymatic attack for this strain. However, enzymatic treatment would be suitable as follow up treatment of mild hydrolysis, where there is oligomeric byproduct of considerable amount generated (25% in the case of virgin PET material; Fig. S11). This substrate would be suitable for biocatalytic depolymerization, as it was shown that crude enzyme preparations from strains that can use BHET as sole source of carbon and energy can efficiently depolymerase PET oligomers (Fig. 2; Figs. S4–S6).

#### 4. Practical applications and future research prospects

Keeping in mind the high volume of newly produced PET materials, it is of high importance to develop mixed mechano/bio-degradation processes to achieve decreased carbon footprint and increase the scope of PET recycling beyond high-grade high-purity PET waste streams. Further research should be directed towards biocatalyst improvement through

enzyme engineering and other optimizations of the biocatalytic process. Namely, the possibility to drive the degradation to completeness and efficiently recover EG and TPA produced should be further explored. The research should also be extended with other types of PET materials, including mixed and postconsumer ones.

## 5. Conclusions

A new *B. subtilis* BPM12 strain with high BHET degradation activity and the ability to attach and form biofilms on PET films was described. A novel carboxylesterase, highly homologous to a previously described intracellular PETase was identified through genome sequencing and overexpressed in both *B. subtilis* BPM12 and 168, resulting in increased BHETase activity. It was also demonstrated that *B. subtilis* BPM12 could serve as an ideal platform for the expression of PETases and other auxiliary enzymes to increase polymer degrading capacity. In pursuit of a combined mechano/bio-degradation approach, mixed mechanical and green chemical hydrolysis recycling was carried out resulting in by-products containing PET oligomers and other partially degraded products. This treatment resulted in substrates that are much more suited for biocatalytic treatment and has the potential to be an important step in achieving more favorable and sustainable routes to advance plastic waste circularity and upcycling.

## Funding

This work was supported by the European Union's Horizon 2020 Research and Innovation Programme under grant agreement No. 870292 (BioICEP) and by the National Natural Science Foundation of China (Nos. 31961133016, 31961133015, and 31961133014). All authors read and approved the final manuscript.

## CRedit authorship contribution statement

**Brana Pantelic:** Methodology, Validation, Investigation, Writing – original draft, Writing – review & editing. **Jeovan A. Araujo:** Methodology, Investigation, Writing – original draft. **Sanja Jeremic:** Methodology, Investigation, Writing – original draft. **Muhammad Azeem:** Methodology, Investigation, Writing – original draft. **Olivia A. Attallah:** Methodology, Investigation, Writing – original draft, Visualization. **Romanos Siaperas:** Investigation, Methodology, Writing – original draft. **Marija Mojicevic:** Conceptualization, Validation, Writing – review & editing. **Yuanyuan Chen:** Investigation, Methodology, Writing – original draft. **Margaret Brennan Fournet:** Conceptualization, Validation, Writing – review & editing. **Evangelos Topakas:** Methodology, Resources, Investigation, Writing – review & editing, Supervision. **Jasmina Nikodinovic-Runic:** Conceptualization, Methodology, Validation, Resources, Writing – review & editing, Supervision, Funding acquisition.

## Declaration of competing interest

The authors declare that they have no known competing financial interests or personal relationships that could have appeared to influence the work reported in this paper.

## Data availability

Data will be made available on request

## Appendix A. Supplementary data

Supplementary material related to this article can be found online at <https://doi.org/10.1016/j.eti.2023.103316>. PET-related model substrates used to investigate the biocatalytic potential of *B. subtilis* BPM12 (Fig. S1); Illustration of the mechanical recycling process using a twin-screw extruder for the fabrication and reprocessing of PET films (Fig. S2). Growth of *B. subtilis* BPM12 compared to *B. subtilis* 168 on LA, MSF, and MSM and blood agar plates (a) and fluorescent microscopy of *B. subtilis* BPM12 under 100 000 x magnification (b). 1.5MER, 2MER and 3MER biotransformation using whole cells of *B. subtilis* BPM12 was monitored via HPLC and TLC (Fig. S4–S6). Growth of *B. subtilis* BPM12 and the knockout mutant *B. subtilis* BPM12  $\Delta bpm12CE$  on MSM plates containing BHET as the sole carbon source b) Growth of *B. subtilis* 168 on MSM plates containing BHET as the sole carbon source; c) Growth of recombinant *Bacillus* strains transformed with BPM12CE on MSM plates containing BHET as the sole carbon source 5 g/L (Fig. S7). General esterase activity of intracellular and extracellular enzyme fractions of recombinant and Wt *B. subtilis* BPM12 and *B. subtilis* 168 (all values are standardized based on protein concentration) (Fig. S8). FTIR spectra of the V-PET, and the reprocessed R<sub>2</sub>-PET and R<sub>5</sub>-PET materials are shown in the wavenumber range 1900–650 cm<sup>-1</sup> (Fig. S9). DSC thermograms of the second heating step of V-PET, R<sub>2</sub>-PET, and R<sub>5</sub>-PET from 30 °C to 275 °C (10 °C/min) under nitrogen atmosphere (30 mL/min) (Fig. S10). The effect of re-extrusion process on the conversion of PET to BHET, MHET and the yield of TPA via MW-assisted hydrolysis using Na<sub>2</sub>CO<sub>3</sub> in ethylene glycol (Fig. S11). FTIR spectra of [a] TPA standard, [b] TPA obtained from V-PET depolymerization, [c] TPA obtained from R<sub>2</sub>-PET depolymerization and [d] TPA obtained from R<sub>5</sub>-PET depolymerization (Fig. S12). Primers used for *bpm12CE* cloning and construction of the knockout mutant *B. subtilis* BPM12  $\Delta bpm12CE$  (Table S1). The ability of *B. subtilis* BPM12 to metabolize different carbohydrates (Table S2). Nucleotide and amino acid sequence of BPM12CE (Table S3). Weight changes after enzymatic degradation of PET films (Table S4).

## References

- Ali, N., Ullah, N., Qasim, M., Rahman, H., Khan, S.N., Sadiq, A., Adnan, M., 2016. Molecular characterization and growth optimization of halo-tolerant protease producing *Bacillus subtilis* strain blk-1.5 isolated from salt mines of Karak, Pakistan. *Extremophiles* 20, 395–402. <http://dx.doi.org/10.1007/s00792-016-0830-1>.
- Azeem, M., Fournet, M.B., Attallah, O.A., 2022. Ultrafast 99% polyethylene terephthalate depolymerization into value added monomers using sequential glycolysis-hydrolysis under microwave irradiation. *Arab. J. Chem.* 15, 103903. <http://dx.doi.org/10.1016/j.arabjc.2022.103903>.
- Badia, J.D., Strömberg, E., Karlsson, S., Ribes-Greus, A., 2012. The role of crystalline, mobile amorphous and rigid amorphous fractions in the performance of recycled poly (ethylene terephthalate) (PET). *Polym. Degrad. Stab.* 97, 98–107. <http://dx.doi.org/10.1016/j.polymdegradstab.2011.10.008>.
- Balci, E., Rosales, E., Pazos, M., Sofuoglu, A., Sanromán, M.A., 2023. Immobilization of esterase from *Bacillus subtilis* on halloysite nanotubes and applications on dibutyl phthalate degradation. *Environ. Technol. Innov.* 30, 103113. <http://dx.doi.org/10.1016/j.eti.2023.103113>.
- Bankevich, A., Nurk, S., Antipov, D., Gurevich, A.A., Dvorkin, M., Kulikov, A.S., Lesin, V.M., Nikolenko, S.I., Pham, S., Prjibelski, A.D., 2012. Spades: A new genome assembly algorithm and its applications to single-cell sequencing. *J. Comput. Biol.* 19, 455–477. <http://dx.doi.org/10.1089/cmb.2012.0021>.
- Benyathir, P., Kumar, P., Carpenter, G., Brace, J., Mishra, D.K., 2022. Polyethylene terephthalate (PET) bottle-to-bottle recycling for the beverage industry: A review. *Polymers* 14 (2366). <http://dx.doi.org/10.3390/polym14122366>.
- Bonifer, K.S., Wen, X., Hasim, S., Phillips, E.K., Dunlap, R.N., Gann, E.R., DeBruyn, J.M., Reynolds, T.B., 2019. *Bacillus pumilus* B12 degrades polylactic acid and degradation is affected by changing nutrient conditions. *Front. Microbiol.* 10 (2548). <http://dx.doi.org/10.3389/fmicb.2019.02548>.
- Buchholz, P., Zhang, H., Perez-Garcia, P., Nover, L.-L., Chow, J., Streit, W.R., Pleiss, J., 2021. Plastics degradation by hydrolytic enzymes: The plastics-active enzymes database-PAZY. *Proteins* 90, 1443–1456. <http://dx.doi.org/10.1002/prot.26325>.
- Chaudhary, S., Surekha, P., Kumar, D., Rajagopal, C., Roy, P.K., 2013. Microwave assisted glycolysis of poly (ethylene terephthalate) for preparation of polyester polyols. *J. Appl. Polym. Sci.* 129, 2779–2788. <http://dx.doi.org/10.1002/app.38970>.
- Chaumeil, P.-A., Müssig, A.J., Hugenholtz, P., Parks, D.H., 2020. Gtdb-tk: A toolkit to classify genomes with the genome taxonomy database. *Oxf. Univ. Press* 36, 1925–1927. <http://dx.doi.org/10.1093/bioinformatics/btz848>.
- Chen, Z., Duan, R., Xiao, Y., Wei, Y., Zhang, H., Sun, X., Wang, S., Cheng, Y., Wang, X., Tong, S., Yao, Y., Zhu, C., Yang, H., Wang, Y., Wang, Z., 2022. Biodegradation of highly crystallized poly(ethylene terephthalate) through cell surface codisplay of bacterial petase and hydrophobin. *Nature Commun.* 13, 7138. <http://dx.doi.org/10.1038/s41467-022-34908-z>.
- Commission, E., 2022. Commission regulation (eu) 2022/1616 of 15 september 2022 on recycled plastic materials and articles intended to come into contact with foods. <https://eur-lex.europa.eu/eli/reg/2022/1616/oj>.
- Contras-Moreira, B., Vinuesa, P., 2013. Get\_homologues, a versatile software package for scalable and robust microbial pangenome analysis. *Appl. Environ. Microbiol.* 79, 7696–7701. <http://dx.doi.org/10.1128/AEM.02411-13>.
- da Costa, A.M., de Oliveira Lopes, V.R., Vidal, L., Nicaud, J.-M., de Castro, A.M., Coelho, M.A.Z., 2020. Poly (ethylene terephthalate)(PET) degradation by *Yarrowia lipolytica*: Investigations on cell growth, enzyme production and monomers consumption. *Process Biochem.* 95, 81–90. <http://dx.doi.org/10.1016/j.procbio.2020.04.001>.
- Diao, J., Hu, Y., Tian, Y., Carr, R., Moon, T.S., 2023. Upcycling of poly (ethylene terephthalate) to produce high-value bio-products. *Cell Rep.* 42, 111908. <http://dx.doi.org/10.1016/j.celrep.2022.111908>.
- Djapovic, M., Milivojevic, D., Ilic-Tomic, T., Lješević, M., Nikolaičits, E., Topakas, E., Maslak, V., Nikodinovic-Runic, J., 2021. Synthesis and characterization of polyethylene terephthalate (PET) precursors and potential degradation products: Toxicity study and application in discovery of novel petases. *Chemosphere* 275, 130005. <http://dx.doi.org/10.1016/j.chemosphere.2021.130005>.
- Earl, A.M., Losick, R., Kolter, R., 2008. Ecology and genomics of *Bacillus subtilis*. *Trends Microbiol.* 16, 269–275. <http://dx.doi.org/10.1016/j.tim.2008.03.004>.
- Edwards, S., León-Zayas, R., Ditter, R., Laster, H., Sheehan, G., Anderson, O., Beattie, T., Mellies, J.L., 2022. Microbial consortia and mixed plastic waste: Pangenomic analysis reveals potential for degradation of multiple plastic types via previously identified PET degrading bacteria. *Int. J. Mol. Sci.* 23 (5612). <http://dx.doi.org/10.3390/ijms23105612>.
- Faraca, G., Martinez-Sanchez, V., Astrup, T.F., 2019. Environmental life cycle cost assessment: Recycling of hard plastic waste collected at danish recycling centres. *Resour. Conserv. Recycl.* 143, 299–309. <http://dx.doi.org/10.1016/j.resconrec.2019.01.014>.
- Ferrero, P., Attallah, O.A., Valera, M.Á., Aleksic, I., Azeem, M., Nikodinovic-Runic, J., Fournet, M.B., 2022. Rendering bio-inert low-density polyethylene amenable for biodegradation via fast high throughput reactive extrusion assisted oxidation. *J. Polym. Environ.* 30, 2837–2846. <http://dx.doi.org/10.1007/s10924-022-02400-w>.
- Gambarini, V., Pantos, O., Kingsbury, J.M., Weaver, L., Handley, K.M., Lear, G., 2021. Phylogenetic distribution of plastic-degrading microorganisms. *mSystems* 6, e01112-20. <http://dx.doi.org/10.1128/mSystems.01112-20>.
- Gangola, S., Joshi, S., Kumar, S., Sharma, B., Sharma, A., 2021. Differential proteomic analysis under pesticides stress and normal conditions in *Bacillus cereus* 2D. *PLoS One* 16, e0253106. <http://dx.doi.org/10.1371/journal.pone.0253106>.
- Gangola, S., Sharma, A., Bhatt, P., Khatri, P., Chaudhary, P., 2018. Presence of esterase and laccase in *Bacillus subtilis* facilitates biodegradation and detoxification of cypermethrin. *Sci. Rep.* 8, 12755. <http://dx.doi.org/10.1038/s41598-018-31082-5>.
- Gangola, S., Sharma, A., Joshi, S., Bhandari, G., Prakash, O., Govarthanam, M., Kim, W., Bhatt, P., 2022. Novel mechanism and degradation kinetics of pesticides mixture using *Bacillus* sp. strain 3C in contaminated sites. *Pest. Biochem. Physiol.* 181, 104996. <http://dx.doi.org/10.1016/j.pestbp.2021.104996>.
- Hanim, C., 2017. Effect of pH and temperature on *Bacillus subtilis* fnc 0059 oxalate decarboxylase activity. *Pak. J. Biol. Sci.* 20, 436–441. <http://dx.doi.org/10.3923/pjbs.2017.436.441>.
- Holland, B.J., Hay, J.N., 2002. The thermal degradation of pet and analogous polyesters measured by thermal analysis–fourier transform infrared spectroscopy. *Polymer* 43, 1835–1847. [http://dx.doi.org/10.1016/S0032-3861\(01\)00775-3](http://dx.doi.org/10.1016/S0032-3861(01)00775-3).
- Huang, X., Cao, L., Qin, Z., Li, S., Kong, W., Liu, Y., 2018. Tat-independent secretion of polyethylene terephthalate hydrolase petase in *Bacillus subtilis* 168 mediated by its native signal peptide. *J. Agricult. Food Chem.* 66, 13217–13227. <http://dx.doi.org/10.1021/acs.jafc.8b05038>.
- Jaeger, K.-E., Kovacic, F., 2014. Determination of lipolytic enzyme activities. In: *Pseudomonas Methods and Protocols*. pp. 111–134. [http://dx.doi.org/10.1007/978-1-4939-0473-0\\_12](http://dx.doi.org/10.1007/978-1-4939-0473-0_12).
- Jaiswal, S., Sharma, B., Shukla, P., 2020. Integrated approaches in microbial degradation of plastics. *Environ. Technol. Innov.* 17, 100567. <http://dx.doi.org/10.1016/j.eti.2019.100567>.
- Jia, Y., Samak, N.A., Hao, X., Chen, Z., Wen, Q., Xing, J., 2022. Hydrophobic cell surface display system of petase as a sustainable biocatalyst for PET degradation. *Front. Microbiol.* 13, 1005480. <http://dx.doi.org/10.3389/fmicb.2022.1005480>.
- Jones, P., Binns, D., Chang, H.-Y., Fraser, M., Li, W., McAnulla, C., McWilliam, H., Maslen, J., Mitchell, A., Nuka, G., 2014. Interproscan 5: Genome-scale protein function classification. *Bioinformatics* 30, 1236–1240. <http://dx.doi.org/10.1093/bioinformatics/btu031>.
- Kawai, F., Kawabata, T., Oda, M., 2019. Current knowledge on enzymatic PET degradation and its possible application to waste stream management and other fields. *Appl. Microbiol. Biotechnol.* 103, 4253–4268. <http://dx.doi.org/10.1007/s00253-019-09717-y>.

- Kenny, S.T., Runic, J.N., Kaminsky, W., Woods, T., Babu, R.P., Keely, C.M., Blau, W., O'Connor, K.E., 2008. Up-cycling of PET (polyethylene terephthalate) to the biodegradable plastic PHA (polyhydroxyalkanoate). *Environ. Sci. Technol.* 42, 7696–7701. <http://dx.doi.org/10.1021/es801010e>.
- Kim, H.T., Kim, J.K., Cha, H.G., Kang, M.J., Lee, H.S., Khang, T.U., Yun, E.J., Lee, D.-H., Song, B.K., Park, S.J., 2019. Biological valorization of poly (ethylene terephthalate) monomers for upcycling waste PET. *Sustain. Chem. Eng.* 7, 19396–19406. <http://dx.doi.org/10.1021/acssuschemeng.9b03908>.
- Kim, H.T., Ryu, M.Hee, Jung, Y.J., Lim, S., Song, H.M., Park, J., Hwang, S.Y., Lee, H.S., Yeon, Y.J., Sung, B.H., 2021. Chemo-biological upcycling of poly (ethylene terephthalate) to multifunctional coating materials. *ChemSusChem* 14, 4251–4259. <http://dx.doi.org/10.1002/cssc.202100909>.
- Kosiorowska, K.E., Moreno, A.D., Iglesias, R., Leluk, K., Mirończuk, A.M., 2022. Production of petase by engineered *Yarrowia lipolytica* for efficient poly (ethylene terephthalate) biodegradation. *Sci. Total Environ.* 846, 157358. <http://dx.doi.org/10.1016/j.scitotenv.2022.157358>.
- Kumari, A., Bano, N., Bag, S.K., Chaudhary, D.R., Jha, B., 2021. Transcriptome-guided insights into plastic degradation by the marine bacterium. *Front. Microbiol.* 2761.
- Kurutos, A., Ilic-Tomic, T., Kamounah, F.S., Vasilev, A.A., Nikodinovic-Runic, J., 2020. Non-cytotoxic photostable monomethine cyanine platforms: Combined paradigm of nucleic acid staining and in vivo imaging. *J. Photochem. Photobiol. A* 397, 112598. <http://dx.doi.org/10.1016/j.jphotochem.2020.112598>.
- Laskar, N., Kumar, U., 2019. Plastics and microplastics: A threat to environment. *Environ. Technol. Innov.* 14, 100352. <http://dx.doi.org/10.1016/j.eti.2019.100352>.
- Li, W., O'Neill, K.R., Haft, D.H., DiCuccio, M., Chetvernin, V., Badretin, A., Coulouris, G., Chitsaz, F., Derbyshire, M.K., Durkin, A.S., 2021. Refseq: Expanding the prokaryotic genome annotation pipeline reach with protein family model curation. *Nucleic Acids Res.* 49, D1020–D1028. <http://dx.doi.org/10.1093/nar/gkaa1105>.
- Liya, S.M., Umesh, M., Nag, A., Chinnathambi, A., Alharbi, S.A., Jhanani, G.K., Shanmugam, S., Brindhadevi, K., 2023. Optimized production of keratinolytic proteases from *Bacillus tropicus* Is27 and its application as a sustainable alternative for dehairing, destaining and metal recovery. *Environ. Res.* 221, 115283. <http://dx.doi.org/10.1016/j.envres.2023.115283>.
- Magalhães, R.P., Cunha, J.M., Sousa, S.F., 2021. Perspectives on the role of enzymatic biocatalysis for the degradation of plastic PET. *Int. J. Mol. Sci.* 22 (11257). <http://dx.doi.org/10.3390/ijms222011257>.
- Maheswaran, B., Al-Ansari, M., Al-Humaid, L., Raj, J.S., Kim, W., Karmegam, N., Rafi, K.M., 2023. In vivo degradation of polyethylene terephthalate using microbial isolates from plastic polluted environment. *Chemosphere* 310, 136757. <http://dx.doi.org/10.1016/j.chemosphere.2022.136757>.
- Makkam, S., Harnnarongchai, W., 2014. Rheological and mechanical properties of recycled PET modified by reactive extrusion. *Energy Procedia* 56, 547–553. <http://dx.doi.org/10.1016/j.egypro.2014.07.191>.
- Manni, M., Berkeley, M.R., Seppely, M., Simão, F.A., Zdobnov, E.M., 2021. Busco update: Novel and streamlined workflows along with broader and deeper phylogenetic coverage for scoring of eukaryotic, prokaryotic, and viral genomes. *Mol. Biol. Evol.* 38, 4647–4654. <http://dx.doi.org/10.1093/molbev/msab199>.
- Martin, M., 2011. Cutadapt removes adapter sequences from high-throughput sequencing reads. *EMBNET. J.* 17, 10–12. <http://dx.doi.org/10.14806/ej.17.1.200>.
- Meyer-Cifuentes, I.E., Öztürk, B., 2021. Mle046 is a marine mesophilic mhetase-like enzyme. *Front. Microbiol.* 12, 693985. <http://dx.doi.org/10.3389/fmicb.2021.693985>.
- Mohan, N., Montazer, Z., Sharma, P.K., Levin, D.B., 2020. Microbial and enzymatic degradation of synthetic plastics. *Front. Microbiol.* 11, 580709. <http://dx.doi.org/10.3389/fmicb.2020.580709>.
- Molitor, R., Bollinger, A., Kubicki, S., Loeschke, A., Jaeger, K.E., Thies, S., 2020. Agar plate-based screening methods for the identification of polyester hydrolysis by *Pseudomonas* species. *Microbiol. Biotechnol.* 13, 274–284. <http://dx.doi.org/10.1111/1751-7915.13418>.
- Mrigwani, A., Thakur, B., Gupatarama, P., 2022. Conversion of polyethylene terephthalate into pure terephthalic acid through synergy between a solid-degrading cutinase and a reaction intermediate-hydrolysing carboxylesterase. *Green Chem.* 24, 6707–6719. <http://dx.doi.org/10.1039/D2GC01965E>.
- Nguyen, L.H., Nguyen, B.-S., Le, D.-T., Alomar, T.S., AlMasoud, N., Ghotekar, S., Oza, R., Raizada, P., Singh, P., Nguyen, V.-H., 2023. A concept for the biotechnological minimizing of emerging plastics, micro- and nano-plastics pollutants from the environment: A review. *Environ. Res.* 216, 114342. <http://dx.doi.org/10.1016/j.envres.2022.114342>.
- Nikolaivits, E., Taxeidis, G., Gkountela, C., Vouyiouka, S., Maslak, V., Nikodinovic-Runic, J., Topakas, E., 2022. A polyesterase from the antarctic bacterium *Moraxella* sp. Degrades highly crystalline synthetic polymers. *J. Hazard. Mater.* 434, 128900. <http://dx.doi.org/10.1016/j.jhazmat.2022.128900>.
- Perera-Costa, D., Bruque, J.M., González-Martín, M.L., Gómez-García, A.C., Vadillo-Rodríguez, V., 2014. Studying the influence of surface topography on bacterial adhesion using spatially organized microtopographic surface patterns. *Langmuir* 30, 4633–4641. <http://dx.doi.org/10.1021/la5001057>.
- PlasticsEurope, 2021. Plastics - the facts 2021. <https://plasticseurope.org/knowledge-hub/plastics-the-facts-2021/>. (Accessed 1 February 2023).
- Qi, X., Ma, Y., Chang, H., Li, B., Ding, M., Yuan, Y., 2021. Evaluation of PET degradation using artificial microbial consortia. *Front. Microbiol.* 12, 778828. <http://dx.doi.org/10.3389/fmicb.2021.778828>.
- Qiu, L., Yin, X., Liu, T., Zhang, H., Chen, G., Wu, S., 2020. Biodegradation of bis (2-hydroxyethyl) terephthalate by a newly isolated *Enterobacter* sp. Hy1 and characterization of its esterase properties. *J. Basic Microbiol.* 60, 699–711. <http://dx.doi.org/10.1002/jobm.202000053>.
- Ragaert, K., Delva, L., Van Geem, K., 2017. Mechanical and chemical recycling of solid plastic waste. *Waste Manag.* 69, 24–58. <http://dx.doi.org/10.1016/j.wasman.2017.07.044>.
- Ribitsch, D., Heumann, S., Trotscha, E., Herrero Acero, E., Greimel, K., Leber, R., Birner-Gruenberger, R., Deller, S., Eiteljoerg, I., Remler, P., 2011. Hydrolysis of polyethyleneterephthalate by p-nitrobenzylesterase from *Bacillus subtilis*. *Biotechnol. Prog.* 27, 951–960. <http://dx.doi.org/10.1002/btpr.610>.
- Roberts, C., Edwards, S., Vague, M., León-Zayas, R., Scheffer, H., Chan, G., Swartz, N.A., Mellies, J.L., 2020. Environmental consortium containing *Pseudomonas* and *Bacillus* species synergistically degrades polyethylene terephthalate plastic. *Mosphere* 5, e01151-20. <http://dx.doi.org/10.1128/mSphere.01151-20>.
- Samak, N.A., Jia, Y., Sharshar, M.M., Mu, T., Yang, M., Peh, S., Xing, J., 2020. Recent advances in biocatalysts engineering for polyethylene terephthalate plastic waste green recycling. *Environ. Int.* 145, 106144. <http://dx.doi.org/10.1016/j.envint.2020.106144>.
- Sammon, C., Yarwood, J., Everall, N., 2000. A FTIR-AIR study of liquid diffusion processes in PET films: Comparison of water with simple alcohols. *Polymer* 41, 2521–2534. [http://dx.doi.org/10.1016/S0032-3861\(99\)00405-X](http://dx.doi.org/10.1016/S0032-3861(99)00405-X).
- Shah, Z., Gulzar, M., Hasan, F., Shah, A.A., 2016. Degradation of polyester polyurethane by an indigenously developed consortium of *Pseudomonas* and *Bacillus* species isolated from soil. *Polym. Degrad. Stab.* 134, 349–356. <http://dx.doi.org/10.1016/j.polymdegradstab.2016.11.003>.
- Shah, Z., Krumholz, L., Aktas, D.F., Hasan, F., Khattak, M., Shah, A.A., 2013. Degradation of polyester polyurethane by a newly isolated soil bacterium, *Bacillus subtilis* strain MZA-75. *Biodegradation* 24, 865–877. <http://dx.doi.org/10.1007/s10532-013-9634-5>.
- Sharma, R., Jasrotia, T., Umar, A., Sharma, M., Sharma, S., Kumar, R., Alkhanjaf, A.A.M., Vats, R., Beniwal, V., Kumar, R., Singh, J., 2022. Effective removal of Pb(ii) and Ni(ii) ions by *Bacillus cereus* and *Bacillus pumilus*: An experimental and mechanistic approach. *Environ. Res.* 212, 113337. <http://dx.doi.org/10.1016/j.envres.2022.113337>.
- Skariyachan, S., Setlur, A.S., Naik, S.Y., Naik, A.A., Usharani, M., Vasist, K.S., 2017. Enhanced biodegradation of low and high-density polyethylene by novel bacterial consortia formulated from plastic-contaminated cow dung under thermophilic conditions. *Environ. Sci. Pollut. Res.* 24, 8443–8457. <http://dx.doi.org/10.1007/s11356-017-8537-0>.



- Souza, C.C.d., Guimarães, J.M., Pereira, S.d.S., Mariúba, L.A.M., 2021. The multifunctionality of expression systems in *Bacillus subtilis*: Emerging devices for the production of recombinant proteins. *Exp. Biol. Med.* 246, 2443–2453. <http://dx.doi.org/10.1177/15353702211030189>.
- Sulaiman, S., Yamato, S., Kanaya, E., Kim, J.-J., Koga, Y., Takano, K., Kanaya, S., 2012. Isolation of a novel cutinase homolog with polyethylene terephthalate-degrading activity from leaf-branch compost by using a metagenomic approach. *Appl. Environ. Microbiol.* 78, 1556–1562. <http://dx.doi.org/10.1128/AEM.06725-11>.
- Suzuki, G., Uchida, N., Tanaka, K., Matsukami, H., Kunisue, T., Takahashi, S., Viet, P.H., Kuramochi, H., Osako, M., 2022. Mechanical recycling of plastic waste as a point source of microplastic pollution. *Environ. Pollut.* 303, 119114. <http://dx.doi.org/10.1016/j.envpol.2022.119114>.
- Teufel, F., Almagro Armenteros, J.J., Johansen, A.R., Gislason, M.H., Pihl, S.I., Tsigirigos, K.D., Winther, O., Brunak, S., von Heijne, G., Nielsen, H., 2022. Signalp 6.0 predicts all five types of signal peptides using protein language models. *Nature Biotechnol.* 40 (7), 1023–1025. <http://dx.doi.org/10.1038/s41587-021-01156-3>.
- Thomsen, T.B., Hunt, C.J., Meyer, A.S., 2022. Influence of substrate crystallinity and glass transition temperature on enzymatic degradation of polyethylene terephthalate (PET). *New Biotechnol.* 69, 28–35. <http://dx.doi.org/10.1016/j.nbt.2022.02.006>.
- Tiso, T., Narancic, T., Wei, R., Pollet, E., Beagan, N., Schröder, K., Honak, A., Jiang, M., Kenny, S.T., Wierckx, N., 2021. Towards bio-upcycling of polyethylene terephthalate. *Metab. Eng.* 66, 167–178. <http://dx.doi.org/10.1016/j.ymben.2021.03.011>.
- Tournier, V., Topham, C., Gilles, A., David, B., Folgoas, C., Moya-Leclair, E., Kamionka, E., Desrousseau, M.-L., Texier, H., Gavalda, S., 2020. An engineered PET depolymerase to break down and recycle plastic bottles. *Nature* 580, 216–219. <http://dx.doi.org/10.1038/s41586-020-2149-4>.
- Uekert, T., DesVeaux, J.S., Singh, A., Nicholson, S.R., Lamers, P., Ghosh, T., McGeehan, J.E., Carpenter, A.C., Beckham, G.T., 2022. Life cycle assessment of enzymatic poly (ethylene terephthalate) recycling. *Green Chem.* 24, 6531–6543. <http://dx.doi.org/10.1039/D2GC02162E>.
- Wang, N., Guan, F., Lv, X., Han, D., Zhang, Y., Wu, N., Xia, X., Tian, J., 2020. Enhancing secretion of polyethylene terephthalate hydrolase petase in *Bacillus subtilis* WB600 mediated by the SP<sub>amy</sub> signal peptide. *Lett. Appl. Microbiol.* 71, 235–241. <http://dx.doi.org/10.1111/lam.13312>.
- Wang, D., Lin, J., Lin, J., Wang, W., Li, S., 2019. Biodegradation of petroleum hydrocarbons by *Bacillus subtilis* BL-27, a strain with weak hydrophobicity. *Molecules* 24 (3021), <http://dx.doi.org/10.3390/molecules24173021>.
- Wei, R., Breite, D., Song, C., Gräsing, D., Ploss, T., Hille, P., Schwardtfefer, R., Matysik, J., Schulze, A., Zimmermann, W., 2019. Biocatalytic degradation efficiency of postconsumer polyethylene terephthalate packaging determined by their polymer microstructures. *Adv. Sci.* 6, 1900491. <http://dx.doi.org/10.1002/advs.201900491>.
- Wei, R., Zimmermann, W., 2017. Biocatalysis as a green route for recycling the recalcitrant plastic polyethylene terephthalate. *Microb. Biotechnol.* 10, 1302. <http://dx.doi.org/10.1111/1751-7915.12714>.
- Wunderlich, B., 1973. *Macromolecular Physics*. vol. I: Crystal Structure, Morphology, Defects Summary. pp. 178–379. <http://dx.doi.org/10.1016/B978-0-12-765601-4.X5001-X>.
- Xi, X., Ni, K., Hao, H., Shang, Y., Zhao, B., Qian, Z., 2021. Secretory expression in *Bacillus subtilis* and biochemical characterization of a highly thermostable polyethylene terephthalate hydrolase from bacterium hr29. *Enzyme Microbial Technol.* 143, 109715. <http://dx.doi.org/10.1016/j.enzmictec.2020.109715>.
- Yang, Y., Malten, M., Grote, A., Jahn, D., Deckwer, W.D., 2007. Codon optimized *Thermobifida fusca* hydrolase secreted by *Bacillus megaterium*. *Biotechnol. Bioeng.* 96, 780–794. <http://dx.doi.org/10.1002/bit.21167>.
- Yi, Y., Kuipers, O.P., 2017. Development of an efficient electroporation method for *Rhizobacterial bacillus mycoides* strains. *J. Microbiol. Meth.* 133, 82–86. <http://dx.doi.org/10.1016/j.mimet.2016.12.022>.
- Yoshida, S., Hiraga, K., Takehana, T., Taniguchi, I., Yamaji, H., Maeda, Y., Toyohara, K., Miyamoto, K., Kimura, Y., Oda, K., 2016. A bacterium that degrades and assimilates poly (ethylene terephthalate). *Science* 351, 1196–1199. <http://dx.doi.org/10.1126/science.aad6359>.